Dalton Transactions

FRONTIER

Materials for Electrochemical Ammonia Synthesis

Ian J. McPherson,[a] Tim Sudmeier, [a] Joshua Fellowes[a] and Shik Chi Edman Tsang [a*]

Received 00th January 20xx,
Accepted 00th January 20xx

DOI: 10.1039/x0xx00000x

www.rsc.org/

Direct electrochemical synthesis of ammonia is proposed as a means of reducing the carbon footprint of the fertiliser industry, as well as providing new opportunities for carbon-free liquid energy storage. We review the current status of research into materials for electrochemical ammonia synthesis and evaluate the reported rates and efficiencies in terms of recent US Department of Energy targets. Surprisingly, development of electrocatalysts has only recently received much attention, and despite a number of promising rates, the target values remain distant. A number of theoretical studies suggest a range of candidate materials yet to be explored.

1. Introduction

Globally, ammonia (NH_3) is one of the most important industrial chemicals, with around 150 million tons synthesised each year.[1] Its primary use is in fertiliser production where it is the source of fixed nitrogen and is so significant for human food production that it is estimated that it accounts for around 50% of all N in the terrestrial N cycle.[2] Recently, however it has also generated interest as a carbon-free energy vector. Its energy density is similar to that of other fuels such as methanol, but can be combusted without releasing CO_2. It contains 17.6% H_2 by weight and can be stored at low pressures and ambient temperatures. The main problem facing NH_3 synthesis, however, is that it is highly energy intensive. NH_3 is commonly produced from N_2 and H_2 at pressures around 200 bar and temperatures around 450°C over a solid iron catalyst.[3] Furthermore, the H_2 is generally produced from methane steam reforming, itself an energy and carbon intensive process. Therefore, to both decrease the significant CO_2 emissions from fertiliser production, and establish NH_3 as a truly sustainable energy vector, the synthesis of NH_3 must be decarbonised, relying only on air and water as feedstocks, and electricity for power.

Electricity can already be used to synthesise NH_3 from air and H_2O simply through electrolytic production of H_2 followed by conventional high pressure and temperature reaction. This system has been suggested to be viable where small scale distributed plants are required. However, the high cost of H_2O electrolysis, coupled with the often low price of methane, make this approach between 1.5-3 times more expensive than conventional synthesis.[4] The goal of electrochemical NH_3 synthesis, in contrast, is to catalyse the direct reaction of N_2 with H_2O to form NH_3 at ambient pressure. This is complicated by the fact that the N_2 molecule is highly inert towards reduction, much more so than the most common electrochemical solvent, H_2O. In principle the reaction can proceed under ambient conditions, as seen in biology, however translating this chemistry into an industrial process while retaining practical rates and efficiencies has proved challenging. Nonetheless, the US Department of Energy has recently announced funding and targets for demonstration electrochemical NH_3 synthesis devices via the ARPA-E REFUEL program, highlighting the desire for progress in this field. In this Frontier article, we examine some of the most promising approaches and the electrode materials behind them.

2. Cells for Electrochemical Ammonia Synthesis

A variety of ways to electrochemically reduce N_2 to NH_3 have been proposed, with conditions ranging from those close to current industrial thermal processes, to aqueous cells operating at ambient temperature and pressure. What the cells have in common is the use of applied voltage, rather than temperature and pressure, to modify the unfavourable position of equilibrium. To do this, cells tend to employ one of four reaction schemes (Figure 1). By far the most common geometry is direct reduction of N_2 at a cathode in the presence of H^+ (Figure 1A). The H is supplied by the electrolyte, either solid or liquid, and is generated at the anode by H_2O (or less commonly H_2) oxidation. Significantly, the theoretical standard potential (where $P_{N2} = P_{NH3} = P_{O2} = 1$) of the N_2/NH_3 couple is slightly more positive than that of H^+/H_2, providing a small window in which N_2 reduction is favoured over H_2 evolution (this window then increasing for P_{NH3} and $P_{O2} < 1$). The second type of cell involves non-proton coupled N_2 reduction at a cathode, forming the nitride ion, N^{3-}, with subsequent reaction of H_2O or H_2 occurring either at the anode or in the electrolyte

[a.] *Address here.*
[b.] *Address here.*
[c.] *Address here.*
† Footnotes relating to the title and/or authors should appear here.
Electronic Supplementary Information (ESI) available: [details of any supplementary information available should be included here]. See DOI: 10.1039/x0xx00000x

(Figure 1B). Interestingly, the reaction between N_2 and H_2 (as opposed to H_2O) is actually spontaneous at room temperature, and only becomes slightly

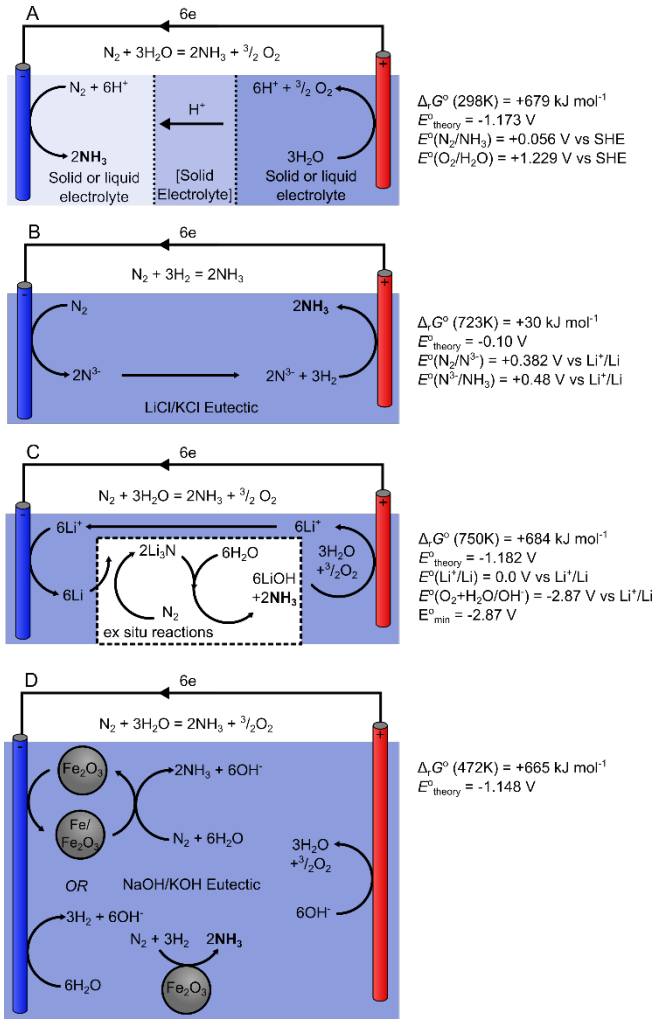

Figure 1 Cells reported for electrochemical NH_3 synthesis. Gibbs energies of reaction are calculated using FactSage,[5] except for B which uses literature values.[6] $E°_{theory} = -\Delta_r G/nF$, where n is the number of electrons and F is the Faraday constant. $E°(O_2/OH^-)$ is from a separate study.[7]

unfavourable at higher temperatures, providing very small theoretical potentials.[6] The third type of cell proposed involves reduction of Li at the cathode, which itself is sufficiently reducing to reduce N_2 to Li_3N. This can subsequently react with a H^+ source, away from the cathode, to generate NH_3 (Figure 1C). While this approach has been suggested as a way to solve the competitive reduction of H_2O to H_2, there is a significant energy penalty for producing a more reduced species as an intermediate.[8] Finally, an alternative approach attempts to combine alkaline water electrolysis with N_2 sparging and a thermal NH_3 catalyst in one pot (Figure 1D). While the results are promising, the mechanism remains unclear.[9] Results reported from all types of cell, along with their operating conditions, are readily summarised by plotting the reported rates and current efficiencies, from recent reviews[10–16] and the primary literature cited herein, as a function of temperature (Figure 2A). The DoE target rate for a viable device is also shown (9.3×10^{-7} mol cm^{-2} s^{-1}), derived from the REFUEL program's target current density (300 mA cm^{-2}) and efficiency (90%). Visualizing the literature in this way highlights a few interesting features of the field:

1. The vast majority of reports fall on or below 10^{-8} mol cm^{-2} s^{-1}. This corresponds to a current density of around 3 mA cm^{-2} at 100% current efficiency and is far short of the DoE target.

2. There is no simple correlation between rate and temperature. Where it has been studied within a particular cell the expected relationship between temperature and rate is observed, however the nature of NH_3 synthesis, as a reversible exothermic reaction, ensures that there is an optimum temperature beyond which the reverse thermal decomposition reaction becomes significant.[17]

3. The majority of reports have current efficiencies less than 10%. This highlights the challenge of not just activating N_2 for reduction, but doing so selectively in the presence of more readily reduced species such as water.

Before proceeding, it is important to note that these reported rates are normalized to a geometric surface area. For planar electrodes this is trivial, however for many technical electrodes such as nanoparticle composites, foams, and felts this area is somewhat arbitrary and may account for significant variations in their intrinsic rates. The low absolute rates also make ammonia quantification challenging; consider that at 1×10^{-8} mol cm^{-2} s^{-1}, the upper end of reported rates, a 1 cm^2 electrode in 50 mL electrolyte would take 1 hour to give an ammonia concentration of only 10 ppm. The error in these measurements is then propagated into the current efficiency, where it can be significantly amplified if low currents are found. To analyse NH_3 concentrations in this range two spectrophotometric detection techniques are commonly used: Nessler's test, which relies on the coordination of NH_3 to K_2HgI_4, giving a yellow complex, and the indophenol method, where NH_3 reacts to form a blue coloured phenolic imide.[19,20] NH_3 ion selective electrodes (ISEs) are also utilised.[21] The spectrophotometric indophenol test has reported limits of detection of 0.02-1 ppm,[18,22,23] while Nessler's reagent has a lower limit of detection of 0.6-1 ppm,[24,25] and modern ISEs of 0.01 ppm according to the manufacturers. Further discussion of the quantification challenges can be found in a recent article by Greenlee, Renner and Foster.[18]

3. Materials for Low Temperature Cells

Low temperature cells fall into two categories: those using a solid state polymer electrolyte, usually Nafion, and those using liquid electrolytes.[12] Note that this review focuses on heterogeneous catalysts, however work on homogeneous catalysis is accelerating,[26] with the recent publication of the first truly electrocatalytic N_2 reduction using a soluble coordination complex showing rates of around 5×10^{-11} mol cm^{-2} s^{-1} with a current efficiency of 19%.[27] For clarity, all the potentials discussed are given versus the reversible hydrogen electrode (RHE). Most reports are based on protonation at the cathode (Figure 1A), although an alternative approach is to

reduce Li^+ ions to metallic Li, which reacts spontaneously with N_2 to form lithium nitride, Li_3N, which goes on to react with H_2 or other hydrogen sources to release NH_3 (Figure 1C).[28] Of the two

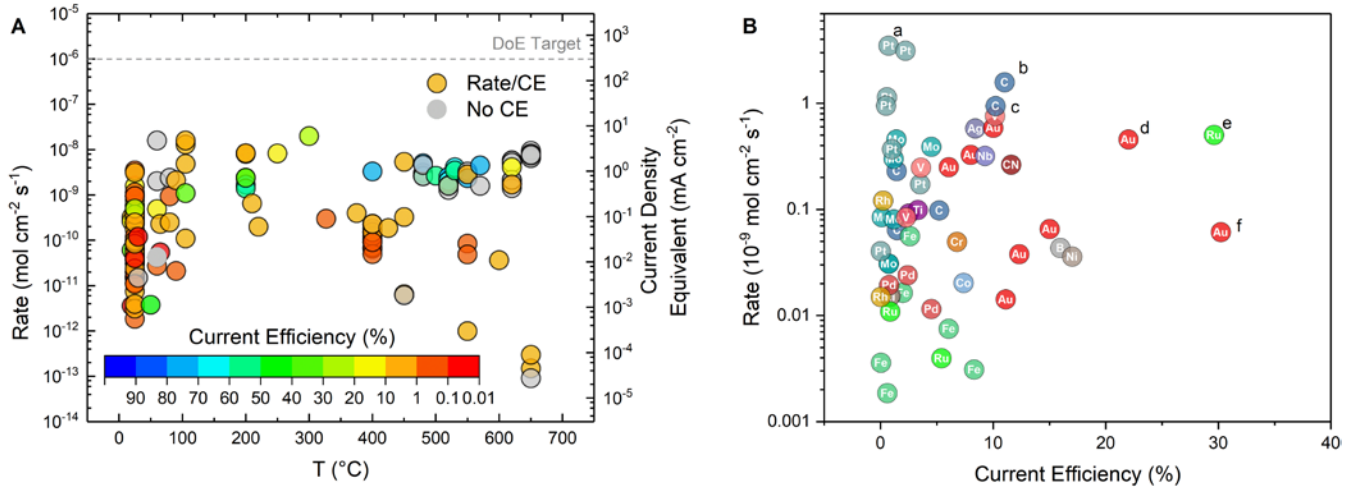

Figure 2 Overview of rates and current efficiencies for electrochemical NH3 synthesis. A: Rate as a function of temperature for all reported cells. Colour indicates current efficiency, grey is used where efficiency data is unavailable. B: Rate as a function of current efficiency for reported aqueous cells around room temperature. Colour and text indicate principle component of catalyst. Labels [a][29][b][30] [c][31] [d][32][e][33] [f][20] are referred to in the text. Data taken from reviews[10–12] as well as literature cited herein.

categories, polymer cells have shown the highest rates and efficiencies. Liu *et al*. report rates around 10^{-8} mol cm^{-2} s^{-1} with surprisingly high efficiencies close to 100% from N_2/H_2 using cells based on composite ceramic/metallic anodes, Nafion electrolyte and a range of quaternary metal oxide cathodes.[34] More commonly, rates around 3×10^{-9} mol cm^{-2} s^{-1} and efficiencies <3% are found for N_2/H_2 (Figure 2B[a]).[29] Peak rates

are seen at 80 °C, corresponding to the maximum in Nafion conductivity.[29,34] For acidic polymers such as Nafion, there also remain questions over their stability in the presence of basic gases like NH_3, although they have been shown to retain some conductivity after NH_3 treatment.[29] A cell based on Pt/C with an anion exchange membrane has also been reported, but shows slower rates than with Nafion.[35]

Low temperature liquid cells based on aqueous electrolytes are perhaps more attractive due to their simplicity and low cost, although they often also include an ion exchange membrane like Nafion to separate anode and cathode solutions. Several classes of catalyst have shown activity in these cells: those based on noble metals, those using transition metals, and those based on nitrogen-doped carbons. The recent surge in reports of catalysts for aqueous ammonia synthesis started with Au nanoparticle systems,[36,37] with the best Au nanoparticle catalyst based on a nanoporous graphitic carbon support.[32] Ammonia production rates of 4.6×10^{-10} mol cm^{-2} s^{-1} at -0.1 V vs RHE and 22% efficiency (Figure 2B[d]) were reported.[32] A range of other Au nanomaterials have been tested and show moderate N_2 reduction rates, and in some cases higher current efficiencies,[30,32,36–38] with 30% reported for hollow Au nanocubes at 20°C (Figure 2B[f]) and up to 40% at 50°C.[20] The relatively high current efficiency may be attributed to the low H_2 evolution reaction (HER) activity of Au compared to other noble metals.[39] In addition, a size effect has been found with sub-nanometer particles being much more active than 6-30 nm particles,[36] and amorphous particles more active than crystalline ones.[38] To capitalise on this, an atomically dispersed Au catalyst supported on C_3N_4 was prepared and also showed high activity as well as excellent atom utilisation.[30] In contrast to thermal catalysis, the reaction on Au is believed to follow an associative mechanism in which addition of hydrogen precedes N-N bond breaking.[37] This is supported by in situ IR evidence of H-N-H and N-N vibrations on Au during N_2 reduction,[40] and the detection of N_2H_4 as a side product on high index Au nanorods.[37] Other noble metals such as Pt, Ru, Pd and Rh also show some activity for N_2 reduction, but often have very low current efficiency due to the competing HER.[39,41–44] This can be mitigated by working at neutral pH, with a current efficiency of 8% at 2.2×10^{-11} mol cm^{-2} s^{-1} reported for Pd/C at +0.1 V vs RHE in pH 7.2 phosphate buffer.[39] Recently, the first experimental examples of atomically dispersed metals on nitrogen-doped carbon (M_1/NC) for electrochemical NH_3 synthesis have emerged, with Au_1/NC and Ru_1/NC exhibiting high current efficiencies.[33,45] Ru_1/NC derived from ZIF-8 shows particular promise (Figure 2B[e]) with a rate of 5.04×10^{-10} mol cm^{-2} s^{-1} at 29.6% efficiency, and interestingly a turnover frequency an order of magnitude higher than that of Ru nanoparticles from the same report.[33]

Despite the progress, more abundant alternatives to noble metal catalysts are desired, and calculations suggest that Mo and Fe are likely to make the most promising catalysts for the associative mechanism.[46] To date only Mo has been tested for aqueous N_2 reduction, with a nanofilm giving a rate of 3.09×10^{-11} mol cm^{-2} s^{-1} at -0.49 V vs RHE where the current efficiency was 0.2%.[47] In addition to pure metals, metal nitrides have also attracted interest for electrochemical ammonia synthesis due to the possibility of a Mars-van Krevelen (MvK) mechanism in which N from the lattice first reacts with H^+ to form NH_3, followed by regeneration of the resulting vacancy via dissociation of N_2.[48,49] Thermal ammonia synthesis via such a mechanism has been demonstrated with the ternary nitride

Co_3Mo_3N,[50] and calculations suggest that the binary rock salt nitrides VN and ZrN should permit such a mechanism to be competitive with HER under aqueous conditions.[48] Recently VN nanosheets as well as nanowires have been synthesised and tested for N_2 reduction activity, with the latter producing $2.48x10^{-10}$ mol cm^{-2} s^{-1} at -0.3 V vs RHE with a current efficiency of 3.58%.[51,52] Similarly, Mo_2N nanorods and MoN nanosheets were prepared with the nanosheets showing a rate of $3x10^{-10}$ mol cm^{-2} s^{-1} at -0.3 V vs RHE and 1.15% current efficiency, confirmed using $^{15}N_2$ labelling.[53,54] Furthermore, loss of nitrogen from this system at -0.3 V vs RHE under Ar supports the presence of a MvK mechanism under aqueous conditions.[53] Analogously, metal oxide and dichalcogenide systems, such as MoO_3, Fe_3O_4, Nb_2O_5 and MoS_2,[14,19,55,56] have been found to be active for N_2 reduction in aqueous media, as well as an amorphous $Bi_4V_2O_{11}/CeO_2$ catalyst, exhibiting a rate of $7.58x10^{-10}$ mol cm^{-2} s^{-1} at -0.2 V vs RHE with a current efficiency of 10.16%.[57]

Pure carbon materials represent a highly attractive class of catalyst, and metal-free N-doped carbons show high activity for several reactions in electrocatalysis, with N_2 reduction being no exception.[58] Materials formed from pyrolysis of the readily prepared zinc-based zeolitic imidazolate framework 8 (ZIF-8) provide a highly disordered but porous and nitrogen-doped carbon framework. These materials show high rates of up to $9x10^{-10}$ mol cm^{-2} s^{-1} at -0.3 V vs RHE with 10% current efficiency in 0.1M KOH (Figure 2B[c]).[31] Interestingly the activity was up to one order of magnitude higher in KOH, as compared to NaOH, suggesting K^+ promotion may occur, but contrary to expectations was seriously inhibited by doping with Fe.[31] N-doped carbon materials are thought to bind metals at the defect sites created by loss of Zn during pyrolysis, and such metal-doped sites have been shown to be active for other electrocatalytic reactions, with calculations suggesting the FeN_3 site,[59] among others,[60,61] may be active for N_2 reduction. Calculation of N_2 adsorption energies by the authors suggests that N_2 binding is only possible at one site, a N_3 moiety consisting of a protonated pyridinic N adjacent to an atomic vacancy. This result reconciles some reports of N_2 reduction activity scaling with pyridinic N content,[62] with those where activity scales with increasing pyrolysis temperature (where pyridinic N content decreases but defect concentration increases).[31] An alternative approach to carbon-based catalysts uses nanospikes prepared from nitrogen-doped carbon which are suggested to act as a so-called 'physical' electrocatalysts, in which the narrow tips of the material generate an increased electric field compared to that of a smooth surface, aiding polarisation of adsorbed N_2 and hence N_2 reduction activity.[63] The material shows the highest room temperature aqueous N_2 reduction rate to date (Figure 2B[b]) at $1.58x10^{-9}$ mol cm^{-2} s^{-1} but with a much larger potential of -1.19 V, and a current efficiency of 11.6%. Carbon nitride materials have also been shown to be active as both a support material,[30] and as the sole catalyst with polymeric carbon nitride reaching rates of $2.64x10^{-10}$ mol cm^{-2} s^{-1} at -0.2V vs RHE with a current efficiency of 11.59%.[64]

4. Synthesis in Molten Salts

While synthesis under ambient conditions is of fundamental interest and remains the long-term goal of much electrochemical NH_3 synthesis research, the cells with the highest rates and efficiencies, and hence the most industrial relevance, are based on molten salts.

Two types of cell have been proposed, one based on LiCl eutectics, the other on hydroxide eutectic/water-in-salt electrolytes, with each supporting distinct chemistry. The LiCl/KCl system is known to permit direct N_2 reduction to the nitride ion, N^{3-}.[65] This has been applied to a cell which combines N_2 reduction over a Ni foam electrode, with N^{3-} ion oxidation in the presence of H_2, also at a Ni foam electrode. The cell was shown to evolve NH_3 at a rate of 3×10^{-9} mol cm^{-2} s^{-1} at 72% efficiency over 40 minutes, although the amount of NH_3 evolved did not exceed the amount of Li_3N precursor added and so the extent of catalysis cannot be determined.[66] A batch process using the same cathode reaction, followed by spontaneous reaction with water and electrochemical oxidation of the resulting (hydr)oxide ions gave a higher rate of 2×10^{-8} mol cm^{-2} s^{-1} with an efficiency of 23%, although again the extent of N_2 reduction was masked by the addition of Li_3N.[66] These systems are unique in that the electrode for N_2 adsorption is different to the one evolving NH_3, allowing for individual optimization of the N_2 reduction and protonation materials. In theory this removes the constraints seen in other cells, where there is an optimum N_2 binding energy due to the scaling relation between the adsorption energies of the initial and final intermediates.[67] However, in practice the electrode material has only received limited attention,[68] perhaps due to the high reactivity of the N^{3-} ion and its tendency to form bulk nitride phases with many metals. The main challenge facing LiCl/KCl cells is the incorporation of water into a continuous (rather than batch) process, not only due to the competition with HER and the hydrolysis of LiCl to release corrosive HCl, but also due to the harsh conditions which sees oxidation of the carbon anode to CO_2 occurring in preference to O_2 evolution.[66]

In contrast, hydroxide eutectics like NaOH/KOH are stable in the presence of H_2O and melt at temperatures below 200°C. Licht *et al*. have demonstrated NH_3 synthesis from N_2 and H_2O in a variety of cells using NaOH/KOH and CsOH electrolytes, achieving rates of up to 2.4×10^{-9} mol cm^{-2} s^{-1} at 35% CE.[9] This is achieved through electrolysis of humidified N_2 between Monel alloy and pure Ni electrodes in a melt containing a large amount of iron oxide nanoparticle catalyst. It is hypothesized that the nanoparticles are reduced at the cathode and go on to react directly with H_2O and N_2 to form NH_3, but the mechanism has not yet been demonstrated conclusively. Recently a hybrid cell combining both eutectics has been reported.[6969] It separates N_2 reduction to N^{3-} in LiCl/KCl, from water splitting in NaOH/KOH with a bipolar Pd membrane. This allows H to be supplied from water without a spontaneous reaction with N^{3-}, thus preventing an increase in required cell voltage. An alternative batch strategy was recently demonstrated in which Li metal was used to reduce N_2 (Figure 1C).[70] First Li was

produced from reduction of molten LiOH/LiCl, before being isolated and reacted with N_2 to form Li_3N, and then water to reform LiOH and release NH_3. No rate was reported, although the total current efficiency was 88.5%. Large overpotentials were required, however, decreasing the energy efficiency of this batch process. In both hydroxide and chloride electrolytes there is evidence that rates can be enhanced by varying the catalyst material,[9,689,68] while strategies from other areas of catalysis such as nanoscale engineering of surface areas have yet to be demonstrated.

5. Solid State Cells

In addition to high temperature liquid cells, ceramic electrolytes operating at temperatures at which H^+ or O^{2-} ion conduction is possible have also been demonstrated for NH_3 synthesis. The fast reaction kinetics seen in melts is retained while the solid state geometry adds easy separation of the cathode and anode gas feeds. Unsurprisingly, the highest rates are observed when H_2 and N_2 are used; 5×10^{-9} mol cm^{-2} s^{-1} was reported at 78% efficiency for a cell operating at 570°C cell based on a $SrCe_{0.95}Yb_{0.05}O_{3-\delta}$ electrolyte and Pd electrodes,[71] and even higher rates are reported for cells at higher temperatures.[10,12] A large number of electrolytes have been tested and the rate remains on the order of 10^{-9} mol cm^{-2} s^{-1} for most of them, regardless of the material.[10,12] When H_2O is used the rates and efficiencies are much lower; a study using $BaZr_{0.8}Y_{0.2}O_{3-\delta}$ electrolytes at 550°C with a range of electrodes found rates of around 10^{-11} mol cm^{-2} s^{-1} at efficiencies <0.5%,[72] this was recently increased to 1.5×10^{-10} mol cm^{-2} s^{-1} at a much lower temperature (400°C) using a $Ce_{0.8}Gd_{0.18}Ca_{0.02}O_{2-\delta}$/carbonate composite electrolyte and a $La_{0.6}Sr_{0.4}Co_{0.2}Fe_{0.8}O_{3-\delta}$-composite cathode, but the efficiency remained low (0.2%).[73] In general there is much less attention paid to the electrodes as catalysts, with many cells using metal pastes such as Ag-Pd. The use of noble metals is not essential, however, and catalysts based on Ni/ceramic composites (cermets e.g. Ni-$BaCe_{0.2}Zr_{0.7}Y_{0.1}O_{2.9}$, Ni-BCZY)[17,74,75], and even pure ceramics, such as $Ba_{0.5}Sr_{0.5}Co_{0.8}Fe_{0.2}O_{3-\delta}$ (BSCF),[76] have been reported to show similar rates.

Electrochemical NH_3 production at higher temperatures is significantly affected by non-electrochemical reactions. For example, at 620°C over a Ni-BCZY cathode co-fed with N_2 and H_2, the net electrochemical rate (i.e. the rate at closed circuit minus the rate at open circuit) was only 40% greater than the open circuit rate.[75] The reverse reaction is also possible and NH_3 production rates start to drop above 600°C due to NH_3 decomposition.[17,74,75] To inhibit decomposition the operating temperature can be decreased by incorporating the ceramic into a composite membrane, where it acts as a solid matrix for a liquid phase such as a molten carbonate. This approach with a $Ce_{0.8}Sm_{0.2}O_{2-\delta}$/ $(Li\text{-}Na\text{-}K)_2CO_3$ composite electrolyte enabled a rate of 5×10^{-9} mol cm^{-2} s^{-1} to be maintained at the lower temperature of 450°C.[77] One challenge facing ceramic cells is the small area of the triple phase boundary formed at the interface between the electrode and the essentially flat surface of the electrolyte. Cathode materials which exhibit H^+ conductivity would allow the three phase boundary to be increased.[10,11] Preparation of ceramic cells is also complicated by their low conductivity, low surface areas and high temperature syntheses, however ultrathin, more conductive electrolytes are now commercially available.[78]

Conclusions and Outlook

Several thousand catalysts were screened in the development of thermal NH_3 synthesis while in comparison relatively few catalysts have been tested systematically for electrochemical activity. Several promising catalysts and electrochemical cells have been developed, however, especially within the past 12 months, with those based on Au, V and nanostructured C appearing the most successful. Pleasingly, the quality of the data reported is increasing, with publications now including many more control experiments, extended stability tests and isotopic labelling studies. Although at present rates remain over an order of magnitude away from DoE targets, continuous progress is being made both in mechanistic understanding of the reaction, and in the development of routes to new materials.

Conflicts of interest

There are no conflicts to declare.

Acknowledgements

The authors acknowledge funding from Siemens PLC, and an EPSRC CASE studentship (TS) and Royal Commission for the Exhibition of 1851 fellowship (TS).

Notes and references

1 J. A. Ober, *Mineral commodity summaries 2018*, Reston, VA, 2018.
2 P. M. Vitousek, J. D. Aber, R. W. Howarth, G. E. Likens, P. A. Matson, D. W. Schindler, W. H. Schlesinger and D. G. Tilman, *Ecol. Appl.*, 1997, **7**, 737–750.
3 M. Appl, *Ammonia : principles and industrial practice*, Wiley-VCH, Weinheim ; Chichester, 1999.
4 R. Bañares-Alcántara, G. Dericks III, M. Fiaschetti, P. Grünewald, J. Masa Lopez, E. Tsang, A. Yang, L. Ye and S. Zhao, *Analysis of Islanded Ammonia-based Energy Storage Systems*, University of Oxford, 2015.
5 C. W. Bale, E. Belise, P. Chartrand, S. A. Decterov, G. Eriksson, A. E. Gheribi, K. Hack, I. H. Jung, Y. B. Kang, J. Melancon, A. D. Pelton, S. Peterson, C. Robelin, J. Sangster and M.-A. Van Ende, *Calphad*, **54**, 35–53.
6 T. Murakami, T. Nishikiori, T. Nohira and Y. Ito, *J. Am. Chem. Soc.*, 2003, **125**, 334–335.
7 O. Takeda, M. Li, T. Toma, K. Sugiyama, M. Hoshi and Y. Sato, *J. Electrochem. Soc.*, 2014, **161**, D820–D823.
8 J. M. McEnaney, A. R. Singh, J. A. Schwalbe, J. Kibsgaard, J. C. Lin, M. Cargnello, T. F. Jaramillo and J. K. Nørskov, *Energy Environ. Sci.*, 2017, **10**, 1621–1630.
9 S. Licht, B. Cui, B. Wang, F.-F. Li, J. Lau and S. Liu, *Science*, 2014, **345**, 637–640.
10 I. A. Amar, R. Lan, C. T. G. Petit and S. Tao, *J. Solid State Electrochem.*, 2011, **15**, 1845–1860.
11 S. Giddey, S. P. S. Badwal and A. Kulkarni, *Int. J. Hydrog. Energy*, 2013, **38**, 14576–14594.

12 V. Kyriakou, I. Garagounis, E. Vasileiou, A. Vourros and M. Stoukides, *Catal. Today*, 2017, **286**, 2–13.
13 M. A. Shipman and M. D. Symes, *Catal. Today*, 2017, **286**, 57–68.
14 J. Han, Z. Liu, Y. Ma, G. Cui, F. Xie, F. Wang, Y. Wu, S. Gao, Y. Xu and X. Sun, *Nano Energy*, , DOI:10.1016/j.nanoen.2018.07.045.
15 N. Cao and G. Zheng, *Nano Res.*, 2018, **11**, 2992–3008.
16 K. Wang, D. Smith and Y. Zheng, *Carbon Resour. Convers.*, 2018, **1**, 2–31.
17 E. Vasileiou, V. Kyriakou, I. Garagounis, A. Vourros, A. Manerbino, W. G. Coors and M. Stoukides, *Solid State Ion.*, 2016, **288**, 357–362.
18 L. F. Greenlee, J. N. Renner and S. L. Foster, *ACS Catal.*, 2018, **8**, 7820–7827.
19 L. Zhang, X. Ji, X. Ren, Y. Ma, X. Shi, Z. Tian, A. M. Asiri, L. Chen, B. Tang and X. Sun, *Adv. Mater.*, 2018, **30**, 1800191.
20 M. Nazemi, S. R. Panikkanvalappil and M. A. El-Sayed, *Nano Energy*, 2018, **49**, 316–323.
21 K. Kim, S. J. Lee, D.-Y. Kim, C.-Y. Yoo, J. W. Choi, J.-N. Kim, Y. Woo, H. C. Yoon and J.-I. Han, *ChemSusChem*, 2018, **11**, 120–124.
22 N. M. Tzollas, G. A. Zachariadis, A. N. Anthemidis and J. A. Stratis, *Int. J. Environ. Anal. Chem.*, 2010, **90**, 115–126.
23 A. Afkhami and R. Norooz-Asl, *J. Braz. Chem. Soc.*, 2008, **19**, 1546–1552.
24 C. Molins-Legua, S. Meseguer-Lloret, Y. Moliner-Martinez and P. Campíns-Falcó, *TrAC Trends Anal. Chem.*, 2006, **25**, 282–290.
25 P. Niedzielski, I. Kurzyca and J. Siepak, *Anal. Chim. Acta*, 2006, **577**, 220–224.
26 S. L. Foster, S. I. P. Bakovic, R. D. Duda, S. Maheshwari, R. D. Milton, S. D. Minteer, M. J. Janik, J. N. Renner and L. F. Greenlee, *Nat. Catal.*, 2018, **1**, 490–500.
27 M. J. Chalkley, T. J. Del Castillo, B. D. Matson and J. C. Peters, *J. Am. Chem. Soc.*, 2018, **140**, 6122–6129.
28 A. Tsuneto, A. Kudo and T. Sakata, *J. Electroanal. Chem.*, 1994, **367**, 183–188.
29 R. Lan, J. T. S. Irvine and S. Tao, *Sci. Rep.*, 2013, **3**, 1145.
30 X. Wang, W. Wang, M. Qiao, G. Wu, W. Chen, T. Yuan, Q. Xu, M. Chen, Y. Zhang, X. Wang, J. Wang, J. Ge, X. Hong, Y. Li, Y. Wu and Y. Li, *Sci. Bull.*, , DOI:10.1016/j.scib.2018.07.005.
31 S. Mukherjee, D. A. Cullen, S. Karakalos, K. Liu, H. Zhang, S. Zhao, H. Xu, K. L. More, G. Wang and G. Wu, *Nano Energy*, , DOI:10.1016/j.nanoen.2018.03.059.
32 H. Wang, L. Wang, Q. Wang, S. Ye, W. Sun, Y. Shao, Z. Jiang, Q. Qiao, Y. Zhu, P. Song, D. Li, L. He, X. Zhang, J. Yuan, T. Wu and G. A. Ozin, *Angew. Chem. Int. Ed.*, , DOI:10.1002/anie.201805514.
33 Z. Geng, Y. Liu, X. Kong, P. Li, K. Li, Z. Liu, J. Du, M. Shu, R. Si and J. Zeng, *Adv. Mater.*, 2018, 1803498.
34 G. Xu and R. Liu, *Chin. J. Chem.*, 2009, **27**, 677–680.
35 J. H. Park, H. C. Yoon, J.-N. Kim, C.-H. Jeong, E.-Y. Jeong, D. S. Yun, H. Yoon, S. H. Park, M.-H. Han and C.-Y. Yoo, *Korean J. Chem. Eng.*, 2018, **35**, 1620–1625.
36 M.-M. Shi, D. Bao, B.-R. Wulan, Y.-H. Li, Y.-F. Zhang, J.-M. Yan and Q. Jiang, *Adv. Mater.*, 2017, **29**, 1606550.
37 D. Bao, Q. Zhang, F.-L. Meng, H.-X. Zhong, M.-M. Shi, Y. Zhang, J.-M. Yan, Q. Jiang and X.-B. Zhang, *Adv. Mater.*, 2017, **29**, 1604799.
38 S.-J. Li, D. Bao, M.-M. Shi, B.-R. Wulan, J.-M. Yan and Q. Jiang, *Adv. Mater.*, 2017, **29**, 1700001.
39 J. Wang, L. Yu, L. Hu, G. Chen, H. Xin and X. Feng, *Nat. Commun.*, , DOI:10.1038/s41467-018-04213-9.
40 Y. Yao, S. Zhu, H. Wang, H. Li and M. Shao, *J. Am. Chem. Soc.*, , DOI:10.1021/jacs.7b12101.
41 H.-M. Liu, S.-H. Han, Y. Zhao, Y.-Y. Zhu, X.-L. Tian, J.-H. Zeng, J.-X. Jiang, B. Y. Xia and Y. Chen, *J. Mater. Chem. A*, 2018, **6**, 3211–3217.
42 M.-M. Shi, D. Bao, S.-J. Li, B.-R. Wulan, J.-M. Yan and Q. Jiang, *Adv. Energy Mater.*, 2018, **8**, 1800124.
43 R. Manjunatha and A. Schechter, *Electrochem. Commun.*, 2018, **90**, 96–100.
44 D. Wang, L. M. Azofra, M. Harb, L. Cavallo, X. Zhang, B. H. R. Suryanto and D. R. MacFarlane, *ChemSusChem*, , DOI:10.1002/cssc.201801632.
45 Q. Qin, T. Heil, M. Antonietti and M. Oschatz, *Small Methods*, 2018, 1800202.
46 J. G. Howalt, T. Bligaard, J. Rossmeisl and T. Vegge, *Phys. Chem. Chem. Phys.*, 2013, **15**, 7785–7795.
47 D. Yang, T. Chen and Z. Wang, *J. Mater. Chem. A*, 2017, **5**, 18967–18971.
48 Y. Abghoui, A. L. Garden, V. F. Hlynsson, S. Björgvinsdóttir, H. Ólafsdóttir and E. Skúlason, *Phys. Chem. Chem. Phys.*, 2015, **17**, 4909–4918.
49 C. D. Zeinalipour-Yazdi, J. S. J. Hargreaves and C. R. A. Catlow, *J. Phys. Chem. C*, , DOI:10.1021/acs.jpcc.5b06811.
50 S. M. Hunter, D. Mckay, R. I. Smith, J. S. J. Hargreaves and D. H. Gregory, *Chem. Mater.*, 2010, **22**, 2898–2907.
51 X. Zhang, R.-M. Kong, H. Du, L. Xia and F. Qu, *Chem. Commun.*, , DOI:10.1039/C8CC00459E.
52 R. Zhang, Y. Zhang, X. Ren, Y. Luo, G. Cui, A. M. Asiri, B. Zheng and X.-P. Sun, *ACS Sustain. Chem. Eng.*, , DOI:10.1021/acssuschemeng.8b01261.
53 L. Zhang, X. Ji, X. Ren, Y. Luo, X. Shi, A. M. Asiri, B. Zheng and X. Sun, *ACS Sustain. Chem. Eng.*, , DOI:10.1021/acssuschemeng.8b01438.
54 X. Ren, G. Cui, L. Chen, F. Xie, Q. Wei, Z. Tian and X. Sun, *Chem. Commun.*, 2018, **54**, 8474–8477.
55 J. Han, X. Ji, X. Ren, G. Cui, L. Li, F. Xie, H. Wang, B. Li and X. Sun, *J. Mater. Chem. A*, 2018, **6**, 12974–12977.
56 Q. Liu, X. Zhang, B. Zhang, Y. Luo, G. Cui, F. Xie and X. Sun, *Nanoscale*, , DOI:10.1039/C8NR04524K.
57 C. Lv, C. Yan, G. Chen, Y. Ding, J. Sun, Y. Zhou and G. Yu, *Angew. Chem. Int. Ed.*, , DOI:10.1002/anie.201801538.
58 W. J. Lee, U. N. Maiti, J. M. Lee, J. Lim, T. H. Han and S. O. Kim, *Chem. Commun.*, 2014, **50**, 6818.
59 X.-F. Li, Q.-K. Li, J. Cheng, L. Liu, Q. Yan, Y. Wu, X.-H. Zhang, Z.-Y. Wang, Q. Qiu and Y. Luo, *J. Am. Chem. Soc.*, 2016, **138**, 8706–8709.
60 C. Choi, S. Back, N.-Y. Kim, J. Lim, Y.-H. Kim and Y. Jung, *ACS Catal.*, , DOI:10.1021/acscatal.8b00905.
61 Y. Cao, Y. Gao, H. Zhou, X. Chen, H. Hu, S. Deng, X. Zhong, G. Zhuang and J. Wang, *Adv. Theory Simul.*, 2018, 1800018.
62 Y. Liu, Y. Su, X. Quan, X. Fan, S. Chen, H. Yu, H. Zhao, Y. Zhang and J. Zhao, *ACS Catal.*, 2018, **8**, 1186–1191.
63 Y. Song, D. Johnson, R. Peng, D. K. Hensley, P. V. Bonnesen, L. Liang, J. Huang, F. Yang, F. Zhang, R. Qiao, A. P. Baddorf, T. J. Tschaplinski, N. L. Engle, M. C. Hatzell, Z. Wu, D. A. Cullen, H. M. Meyer, B. G. Sumpter and A. J. Rondinone, *Sci. Adv.*, 2018, **4**, e1700336.
64 C. Lv, Y. Qian, C. Yan, Y. Ding, Y. Liu, G. Chen and G. Yu, *Angew. Chem. Int. Ed.*, , DOI:10.1002/anie.201806386.
65 T. Goto and Y. Ito, *Electrochimica Acta*, 1998, **43**, 3379–3384.
66 T. Murakami, T. Nohira, T. Goto, Y. H. Ogata and Y. Ito, *Electrochimica Acta*, 2005, **50**, 5423–5426.
67 J. H. Montoya, C. Tsai, A. Vojvodic and J. K. Nørskov, *ChemSusChem*, 2015, **8**, 2180–2186.
68 K. Kim, J.-N. Kim, H. C. Yoon and J.-I. Han, *Int. J. Hydrog. Energy*, 2015, **40**, 5578–5582.
69 Y. Ito, T. Nishikiori and H. Tsujimura, *Faraday Discuss*, 2016, **190**, 307–326.
70 J. M. McEnaney, A. R. Singh, J. A. Schwalbe, J. Kibsgaard, J. Lin, M. Cargnello, T. Jaramillo and J. K. Nørskov, *Energy Env. Sci*, , DOI:10.1039/C7EE01126A.
71 G. Marnellos and M. Stoukides, *Science*, 1998, **282**, 98–100.
72 D. S. Yun, J. H. Joo, J. H. Yu, H. C. Yoon, J.-N. Kim and C.-Y. Yoo, *J. Power Sources*, 2015, **284**, 245–251.
73 I. A. Amar, R. Lan, J. Humphreys and S. Tao, *Catal. Today*, 2017, **286**, 51–56.
74 E. Vasileiou, V. Kyriakou, I. Garagounis, A. Vourros, A. Manerbino, W. G. Coors and M. Stoukides, *Top. Catal.*, 2015, **58**, 1193–1201.
75 E. Vasileiou, V. Kyriakou, I. Garagounis, A. Vourros and M. Stoukides, *Solid State Ion.*, 2015, **275**, 110–116.
76 W. B. Wang, X. B. Cao, W. J. Gao, F. Zhang, H. T. Wang and G. L. Ma, *J. Membr. Sci.*, 2010, **360**, 397–403.
77 I. A. Amar, C. T. G. Petit, L. Zhang, R. Lan, P. J. Skabara and S. Tao, *Solid State Ion.*, 2011, **201**, 94–100.
78 S. Robinson, A. Manerbino, W. Grover Coors and N. P. Sullivan, *Fuel Cells*, 2013, **13**, 584–591.

